Ultra-Antireflective Electrodeposited Plasmonic and PEDOT Nanocone Array Surfaces

*Han Wai Millie Fung, Seulgi So, Kellen Kartub, Gabriel Loget† and Robert M. Corn**

Department of Chemistry, University of California-Irvine, Irvine, CA 92697, USA.

†Present Address: Institut des Sciences Chimiques de Rennes, UMR 6226 CNRS, Université de Rennes 1, Campus de Beaulieu, 35042 Rennes Cedex, France.

Corresponding Author

*Robert M. Corn: rcorn@uci.edu

Abstract

Novel broadband ultra-antireflective surfaces were created via the electrodeposition of a nanostructured zinc oxide thin film onto conductive, light absorbing periodic nanocone arrays. Nanocone arrays of (i) fluorinated ethylene propylene (FEP) coated with a 50 nm plasmonic gold thin film and (ii) the electroactive polymer poly(3,4-ethylenedioxythiophene (PEDOT) exhibited a very low broadband reflectivity of less than 0.1% from 475 nm to 800 nm at a wide range of incident angles after the electrodeposition of a nanostructured ZnO thin film onto the surface. SEM images reveal the formation of ZnO nanoflowers and nanorods on both nanocone array surfaces; these additional ZnO nanostructures enhance the coupling of the incident visible light into the absorptive gold or PEDOT nanocones to significantly reduce the reflectivity of these surfaces. The ZnO-coated nanocone array surfaces also exhibited an enhanced photoreactivity for the oxidative degradation of methylene blue, suggesting their potential to be used as self-cleaning antireflective surfaces.

KEYWORDS broadband antireflectivity; nanocone arrays; plasmonic; zinc oxide; nanostructured electrodeposition

TOC Graphic

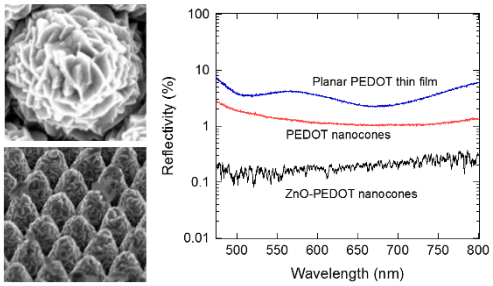

Nanostructured array surfaces can provide excellent broadband antireflectivity over a wide range of optical wavelengths and incident angles, and have been incorporated as optical coatings into various devices such as solar cells,[1,2] photodetectors,[3] and electroreflective windows.[4] Traditionally, arrays of transparent zinc oxide nanostructures have been fabricated by chemical vapor deposition[5-7] or electrochemical methods[8-11] to create a graded interfacial refractive index coating that increases the transmittance of silicon solar cell devices by reducing the reflectivity of the device surface down to approximately 2-5%.[12-14] However, when a transparent nanostructured ZnO coating is used in a hierarchical fashion with a subwavelength periodic array of an absorbing material,[15,16] an even better broadband antireflective surface can be created. Recently, we have demonstrated the fabrication of periodic absorptive nanocone arrays of gold-coated fluorinated ethylene propylene (FEP)[17] and the electroactive polymer poly(3,4-ethylenedioxythiophene) (PEDOT);[18] our large area fabrication process employs the oxygen plasma etching of a square centimeter scale polymer substrate or thin film that has been covered with a colloidal monolayer of polystyrene (PS) beads. The resultant plasmonic gold and PEDOT nanocone array surfaces both exhibited excellent broadband antireflectivity; for the gold surfaces a reflectivity of less than 1% was observed from 475nm to 800 nm over a wide range of

incident angles.[17] In this paper, we show that the reflectivity for both the gold and PEDOT nanocone arrays can be reduced even further by the electrodeposition of a nanostructured ZnO coating; for the PEDOT nanocone arrays; up to a 10-fold reduction in reflectivity is observed with reflectivities of 0.1 to 0.2% throughout the visible spectral region while transmitting from 2 to 10%. The ultra-antireflective ZnO-coated nanocone array surfaces are characterized with SEM, XRD, and XPS, and additionally are shown to be photocatalytic and thus potential self-cleaning surfaces. Moreover, the PEDOT nanocone arrays are electro-reflective and thus can be incorporated into electro-optical devices. These ultra-antireflective surfaces are extremely useful in applications where reflections must be absolutely minimized; examples include laser optics and anti-glare coatings for mirrors displays, cameras and lenses.

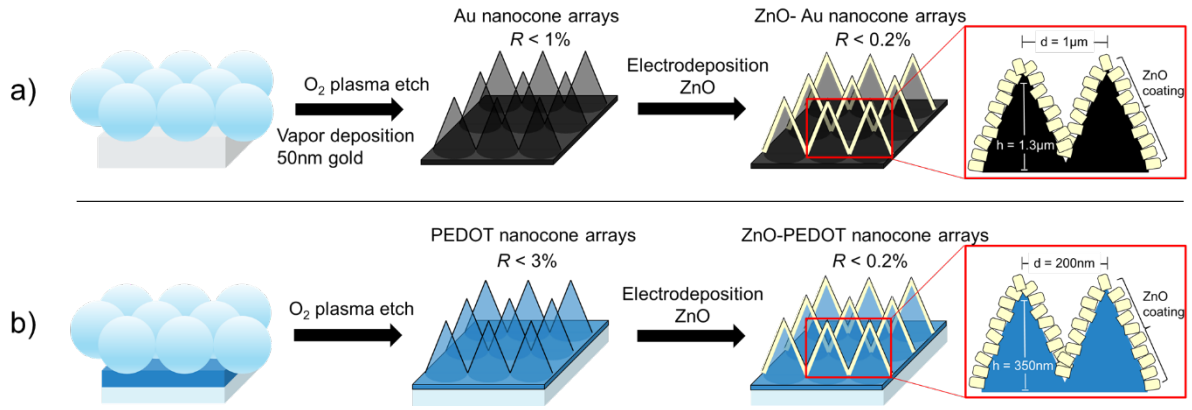

Figure 1. Schematic illustration of the fabrication of ultra-antireflective ZnO-coated nanocone arrays using a) Au nanocone arrays and b) PEDOT nanocone arrays.

Large scale periodic ZnO-coated nanocone array surfaces (areas on the order of cm^2) were fabricated using a combination of colloidal lithography, plasma etching, vapor deposition, and electrochemistry. As shown in the scheme in Figure 1, the simultaneous oxygen plasma

etching of a hexagonally closed packed monolayer of PS bead colloidal mask spincoated onto either a FEP substrate or a PEDOT thin film created periodic nanocone arrays; nanocone formation occurs due to the simultaneous etching of both the PS colloidal mask and the polymer underneath. The aspect ratio of the resultant nanocones can be optimized: the size of the PS beads controls the distance between the nanocones, while the O_2 plasma etching time controls the height of the nanocones. For the FEP nanocone arrays, PS beads with a 1μm diameter were used as the colloidal mask, whereas for the PEDOT nanocone arrays, PS beads with a 0.2 μm diameter were used as the colloidal mask. In the next step, the FEP nanocone arrays were made conductive via vapor deposition of a 50 nm layer of gold, whereas the PEDOT nanocone arrays were already conductive. Finally, an additional nanostructured ZnO coating was created using electrochemistry. In this approach, 0.1 M of aqueous zinc nitrate ($Zn(NO_3)_2$) at pH 4.0 was used as the plating solution, and electrodeposition occurred at 70°C for 150 seconds at an anodic potential of -0.9 V against a Ag/AgCl reference electrode. The mechanism of the ZnO electrodeposition process is described as follows: At a sufficiently negative applied potential, NO_3^- ions are reduced to generate OH^- ions (eqn 1). The OH^- and the Zn^{2+} ions then result in the precipitation of ZnO onto the Au or PEDOT nanocone array working electrode (eqn 2).[8-11]

$$NO_3^- + H_2O + 2e^- \rightarrow NO_2^- + 2OH^- \quad (1)$$

$$Zn^{2+} + 2OH^- \rightarrow ZnO \downarrow + H_2O \quad (2)$$

Nanostructured polycrystalline ZnO films were formed directly from this facile electrodeposition method, without the need for a subsequent thermal annealing step. The electrodeposition process was monitored by chronoamperometry of the working electrode (either the Au or PEDOT nanocone arrays), as shown in Supporting Information Figure S1. The initial increase and the subsequent gradual decrease of the absolute current density over time indicated that the

conductive nanocone array surfaces became slightly passivated with the addition of a ZnO thin film.

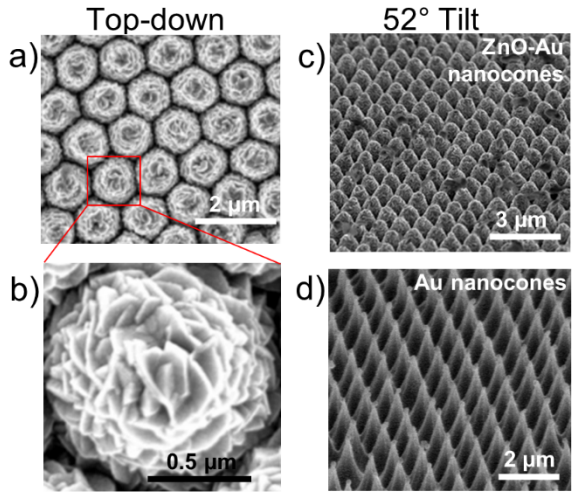

Figure 2. SEM images of ZnO-Au nanocone arrays from top-down (a, b) and tilted (c, d) views.

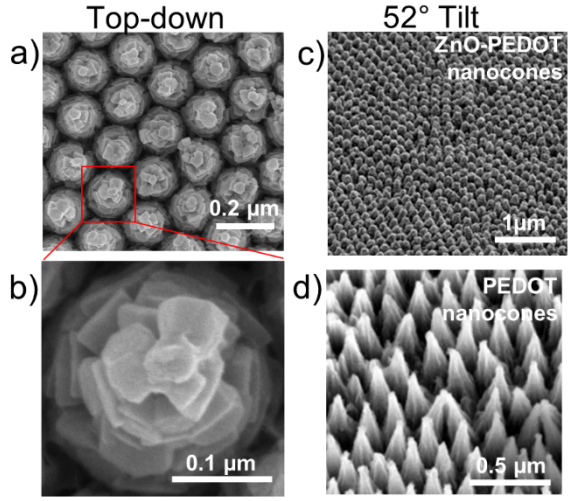

Figure 3. SEM images of ZnO-PEDOT nanocone arrays from top-down (a, b) and tilted (c, d) views.

The morphology of the ZnO-coated nanocone arrays was characterized using a combination of scanning electron microscopy (SEM), X-ray diffraction (XRD), and X-ray photoelectron spectroscopy (XPS). SEM images from Figures 2 and 3 show top-down and tilted views of the nanostructured ZnO thin film on Au and PEDOT nanocone arrays, respectively. From Figure 2a, c and Figure 3a, c, it can be seen that hexagonally close packed ZnO-coated nanocones were created on a large scale, extending over an area of several square microns. Comparing the heights of the ZnO-coated nanocones with Au and PEDOT nanocones from Figure 2d and 3d, respectively, using SEM measurements, we determined that a 25 nm of ZnO coating was formed during electrodeposition. Figures 2b and 3b showed a high magnification image of an individual ZnO-coated Au and PEDOT nanocone, respectively, where we could see the individual ZnO nanostructures formed on the surface. XRD analysis (as shown in Supporting Information Figure S2) revealed a polycrystalline wurzite crystal structure that grew primarily in the <002> direction, which is consistent with previous work in ZnO electrodeposition.[9,10] We also confirmed that ZnO was formed on both the Au and PEDOT nanocone array surfaces via XPS, shown in the Supporting Information Figure S3.

Additionally, the photocatalytic activity of the ZnO-coated nanocone arrays was also characterized via the oxidative degradation of a methylene blue (MB) dye under UV conditions. As shown in Supporting Information Figure S4a, we evaluated the relative concentration of MB over time using UV-Vis spectroscopy under the following catalytic conditions: exposure to a ZnO-coated nanocone array surface, ZnO thin film surface, and no catalyst. As shown in Supporting Information Figure S4b, 11±1% of the MB remained in solution after 14 minutes of exposure to a planar ZnO thin film surface, whereas 0±1% of the MB remained in solution after 14 minutes of exposure to a ZnO-coated nanocone array surface. This demonstrates that since the

high surface area of the ZnO-coated nanocone arrays allowed for increased UV absorption,[19,20] the ZnO-coated nanocone array surface performed better as a photocatalyst compared to a planar ZnO thin film surface during MB degradation, and may find applications as self-cleaning surfaces.

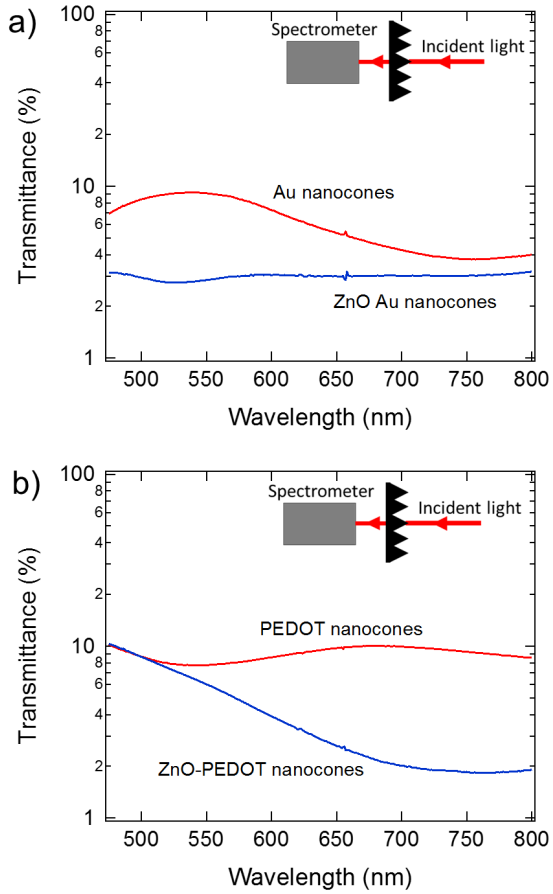

Figure 4. Transmittance spectra for a) Au and ZnO-Au nanocone arrays and b) PEDOT and ZnO-PEDOT nanocone arrays. The decrease in transmittance for the ZnO-coated nanocone arrays indicates the ZnO enhances the performance of the light absorbing material underneath (Au or PEDOT). The inserted schematic shows the optical setup used for transmittance measurements.

Optical characterization revealed that the ZnO-coated nanocone array surfaces became more light absorbing and more antireflective than just Au and PEDOT nanocone arrays over a wide range of optical wavelengths from 475 nm to 800 nm. In Figure 4, the percent transmittance measurements of the ZnO-coated nanocone arrays compared to just Au and PEDOT nanocone arrays are shown. For all transmittance measurements, a halogen lamp was used as a white light source. The light was directed onto the nanocone array surface at a normal angle of incidence, and the transmitted light from the nanocone array surface was measured using a UV-Vis spectrometer. As shown in Figure 4a, the transmittance measurements of the Au nanocone arrays were $T = 10\%$ or less across the 475 nm to 800 nm spectral range, indicating strong light absorption. However, the transmittance measurements of the ZnO-Au nanocone arrays were $T = 3\%$ in the same spectral range, indicating up to a 3-fold improvement in the light absorbing ability of the Au nanocone arrays when they are decorated with ZnO nanostructures on the surface. Similarly, the transmittance measurements for the PEDOT nanocone arrays were $T = 10\%$ across the 475 nm to 800 nm spectral range, but decrease to $T = 2\%$ for the ZnO-PEDOT nanocone arrays from $\lambda = 650$ nm to 800 nm, indicating up to a 5-fold improvement in the light absorbing ability of the ZnO-PEDOT nanocone arrays across a wide range of optical wavelengths. A possible explanation for the increased light absorbance of the ZnO-coated nanocone arrays is that the ZnO nanostructures on the surface are acting as optical couplers; although ZnO itself does not absorb in the 475 nm to 800 nm wavelength range, the coupling between the ZnO nanostructures and the light absorbing material underneath (either Au or PEDOT) enhances the light trapping capacity of the nanocone arrays and increases their effective absorption bands.[21,22]

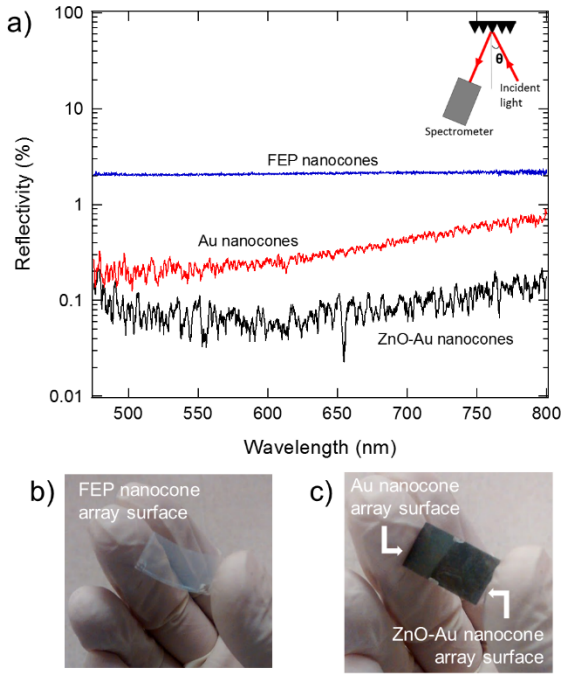

Figure 5. Reflectivity spectra for various nanocone array structures composed of a FEP substrate. The ZnO-coated gold nanocone array surfaces exhibit superior antireflective properties. The inserted schematic shows optical setup used for reflectivity measurements. Reflectivity measurements are shown for incident light hitting the nanocone array surfaces at a nearly normal angle of incidence (θ) at 8°.

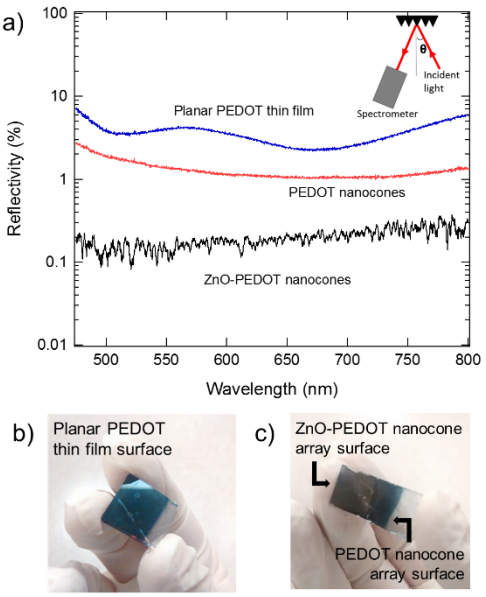

Figure 6. Reflectivity spectra for various nanocone array structures composed of a PEDOT substrate. The ZnO-coated PEDOT nanocone array surfaces exhibit enhanced antireflective properties. The inserted schematic shows optical setup used for reflectivity measurements. Reflectivity measurements are shown for incident light hitting the surfaces at a nearly normal angle of incidence (θ) at 8°.

The most striking effect of the addition of a nanostructured ZnO thin film onto the nanocone arrays was a significant increase in broadband antireflectivity of these surfaces. In our previous papers, we fabricated Au nanocone array surfaces that are less than 0.7% reflective at a nearly normal angle of incidence ($\theta = 8°$) from $\lambda = 475$ nm to 800 nm,[17] and we also recently fabricated PEDOT nanocone array surfaces that were less than 3% reflective over the same wavelength range.[18] The antireflective behavior of the ZnO-coated nanocone arrays are shown in Figures 5 and 6. For the reflectivity measurements, the optical setup with a halogen lamp white light source at either angle of incidence $\theta = 8°$, 45°, or 67° was used as shown in the inset of

Figure 5, and a silver mirror was used as reference calibration. In Figure 5a, reflectivity measurements are shown for ZnO-coated Au nanocones in comparison to Au and FEP nanocone arrays at $\theta = 8°$. The FEP nanocone arrays, visually matte white as seen in the photograph from Figure 5b, exhibited broadband antireflective properties at 2% reflective ($R = 2\%$) from $\lambda = 475$ nm to 800 nm. The addition of a 50 nm light absorbing gold thin film on the FEP nanocone arrays created a visually dark Au nanocone array surface (photograph shown in Figure 5c); the percent reflectivity decreased to less than $R = 0.7\%$ over the same spectral range, as seen in Figure 5a. Electrodeposition of a nanostructured ZnO film created ZnO-Au nanocone arrays that were visually even blacker than the Au nanocone arrays (Figure 5c), and the reflectivity measurements for the ZnO-Au nanocone arrays were reduced to $R < 0.3\%$ from 450 nm to 750 nm, with $R_{min} = 0.05\%$. We attribute the very low reflectivity exhibited by the ZnO-Au nanocone array surfaces to (i) increased coupling into the nanocone absorption bands by the ZnO nanostructures,[21,22] (ii) increased light scattering by the ZnO nanostructures, and (iii) an increase in the graded interfacial complex refractive index created by addition of the ZnO film to the nanocones.[23-25] Even more striking results were obtained for the PEDOT nanocone array surfaces. Visually, we observed once again from the photograph shown in Figure 6c that the ZnO-PEDOT nanocone arrays were blacker than the PEDOT nanocone arrays. In Figure 6a, reflectivity measurements showed that while the PEDOT nanocone arrays were less than 3% reflective ($R < 3\%$) from 450 nm to 800 nm at $\theta = 8°$, the ZnO-PEDOT nanocone arrays were over an order of magnitude less reflective at $R < 0.2\%$ over the same spectral range. Since this reflectivity spectrum is very similar to the spectra for ZnO-coated gold FEP arrays, the mechanism for the suppressed reflectivity of the ZnO-PEDOT nanocone arrays must be similar and thus can also be explained by increased light absorption and increased light scattering of the

ZnO nanostructured surface. Finally, a very similar decrease in broadband reflectivity was also obtained for both ZnO-Au and ZnO-PEDOT nanocone arrays at higher angles of incidence (θ = 45° and θ = 67.5°), as shown in Figure 7.

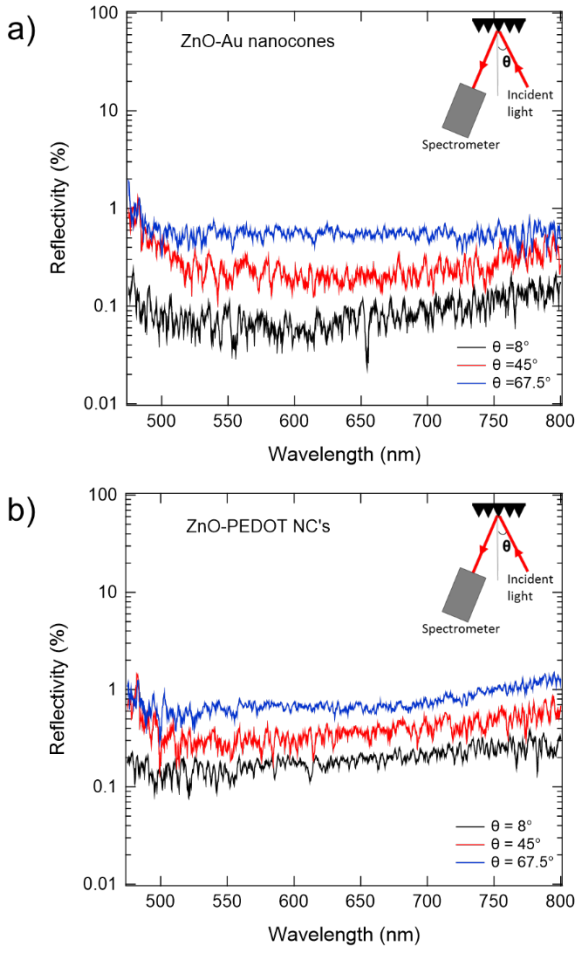

Figure 7. Reflectivity spectra for a) ZnO-Au nanocone arrays and b) ZnO-PEDOT nanocone arrays at various angles of incidence (θ), at 8° (black), 45° (red), and 67.5° (blue). The inserted schematic shows the optical setup used for reflectivity measurements.

In conclusion, we have demonstrated that electrodeposition of nanostructured ZnO films

onto both FEP-Au and PEDOT periodic nanocone arrays creates surfaces with excellent broadband antireflectivity that are less than 0.2% reflective over a large optical wavelength range of 475 nm to 800 nm. These surfaces are up to 10 times more antireflective than the nanocone arrays without the ZnO film. The nanostructured ZnO coating enhances the graded interfacial complex refractive index created by the FEP-Au or PEDOT nanocone arrays that is responsible for the antireflectivity, and additionally increases both the scattering and coupling efficiency of incident light into the absorptive nanocones. The ZnO nanostructures created from this process also increase the surface area of the nanocone arrays, resulting in a higher surface reactivity for potential photocatalytic applications. Finally, the enhanced coupling of incident light into the light absorbing FEP-Au or PEDOT nanocones from the ZnO film also enhances the optical absorption properties of the nanocone arrays. Since these ZnO-coated nanocone array surfaces are easy to fabricate over large surface areas on flexible substrates, they should be easily implemented in various potential applications such as highly antireflective self-cleaning surface coatings for displays and solar panels.

Supporting Information

The following are available free of charge: (i) experimental details of the characterization of the ZnO-coated nanocone arrays' morphology, composition, and photocatalytic degradation of methylene blue, (ii) electrochemical data of ZnO thin film electrodeposition, (iii) XRD and XPS spectra of ZnO-coated nanocone arrays, (iv) UV-Vis spectra of relative MB concentrations under

various photocatalytic conditions, and (v) reflectivity spectra of ZnO-coated nanocone arrays at incident angles of 8°, 45°, and 67.5°.

Notes

The authors declare no competing financial interests.

ACKNOWLEDGMENTS

This work was supported by the National Science Foundation through grant CHE-1403506.

REFERENCES

(1) Chen, Y.; Xu, Z.; Gartia M. R.; Whitlock, D.; Lian, Y.; Liu, G. L. Ultrahigh Throughput Silicon Nanomanufacturing by Simultaneous Reactive Ion Synthesis and Etching. *ACS Nano* ***2011***, 5, 8002-8012.

(2) He, J.; Gao, P.; Liao, M.; Yang, X.; Ying, Z.; Zhou, S.; Ye, J.; Cui, Y. Realization of 13.6% Efficiency on 20 um Thick Si/Organic Hybrid Heterojunction Solar Cells via Advanced Nanotexturing and Surface Recombination Suppression. *ACS Nano* ***2015***, 9, 6522-6531.

(3) Fujii, T.; Gao, Y.; Sharma, R.; Hu, E. L.; DenBaars, S. P.; Nakamura, S. Increase in the Extraction Efficiency of GaN-Based Light-Emitting Diodes via Surface Roughening. *Appl. Phys. Lett*. ***2004***, 84, 855-857.

(4) Araki, S.; Nakamura, K.; Kobayashi, K.; Tsuboi, A.; Kobayashi, N. Electrochemical Optical-Modulation Device with Reversible Transformation Between Transparent, Mirror, and Black. *Adv. Mater*. ***2012***, 24, OP122-OP126

(5) Wu, J. J.; Liu, S. C.; Low-Temperature Growth of Well-Aligned ZnO Nanorods by Chemical Vapor Deposition. *Adv. Mat*. ***2002***, 14, 215-217.

(6) Peiro, A. M.; Ravirajan, P.; Govender, K.; Boyle, D. S.; O'Brien, P.; Bradley, D. D. C.; Nelson, J.; Durrant, J. R. Hybrid Polymer/Metal Oxide Solar Cells Based on ZnO Columnar Structures. *J. Mater. Chem*. ***2006***, 16, 2088-2096.

(7) Montenegro, D.N.; Souissi, A.; Martinez-Tomas, C.; Munoz-Sanjose, V.; Sallet, V. Morphology Transitions in ZnO Nanorods Grown by MOCVD. *J. Cryst. Growth* ***2012***, 359, 122-128.

(8) Wahab, R.; Ansari, S. G.; Kim, Y. S.; Seo, H. K.; Kim, G. S.; Khang, G.; Shin, H-S. Low Temperature Solution Synthesis and Characterization of ZnO Nano-Flowers. *Mater. Res. Bull*. ***2007***, 42, 1640-1648.

(9) Illy, B. N.; Cruickshank, A. C.; Schumann, S.; Da Campo, R.; Jones, T. S.; Heutz, S.; McLachian, M. A.; McComb, D. W.; Riley, D. J.; Ryan, M. P. Electrodeposition of ZnO Layers for Photovoltaic Application: Controlling Film Thickness and Orientation. *J. Mater. Chem*. ***2011***, 21, 12949-12957.

(10) Sun, S.; Jiao, S.; Zhang, K.; Wang, D.; Gao, S.; Li, H.; Wang, J.; Yu, Q.; Guo, F.; Zhao, L. Nucleation Effect and Growth Mechanism of ZnO Nanostructures by Electrodeposition from Aqueous Zinc Nitrate Baths. *J. Cryst. Growth* ***2012***, 359, 15-19.

(11) Klochko, N. P.; Khrypunov, G. S.; Myagchenko, Y. O.; Melnychuk, E. E.; Kopach, V. R.; Klepikova, K. S.; Lyubov, V. M.; Kopach, A. V. Electrodeposited Zinc Oxide Arrays with the Moth-Eye Effect. *Semiconductors* ***2014***, 48, 531-537.

(12) Tsui, K.; Lin, Q.; Chou, H.; Zhang, Q.; Fu, H,; Qi, P. Low-Cost, Flexible, and Self-Cleaning 3D Nanocone Anti-Reflection Films for High-Efficiency Photovoltaics. *Adv. Mater*. ***2014***, 26, 2805-2811.

(13) Leem, J. W.; Kim, S.; Lee, S. H.; Rogers, J. A.; Kim, E.; Yu, J. S. Efficiency Enhancement of Organic Solar Cells Using Hydrophobic Antireflective Inverted Moth-Eye Nanopatterned PDMS Film. *Adv. Energy Mater*. ***2014***, 4, 1-7.

(14) Wang, Y.; Lu, N.; Xu, H.; Shi, G.; Xu, M.; Lin, X.; Li, H.; Wang, W.; Qi, D.; Lu, Y.; Chi, L. Biomimetic Corrugated Silicon Nanocone Arrays for Self-Cleaning Antireflection Coatings. *Nano Res*. ***2010***, 3, 520-527.

(15) Garnett, E.; Yang, P.; Ordered Arrays of Dual-Diameter Nanopillars for Maximized Optical Absorption. *Nano. Lett*. ***2010***, 10, 1082-1087.

(16) Wilson, S. J.; Hutley, M.C. The Optical Properties of 'Moth Eye' Antireflection Surfaces. *Optica Acta* ***1982***, 29, 993-1009.

(17) Toma, M.; Loget, G.; Corn, R. M.; Fabrication of Broadband Antireflective Plasmonic Gold Nanocone Arrays on Flexible Polymer Films. *Nano Lett*. ***2013***, 13, 6164-6169.

(18) So, S.; Fung, H. W. M.; Kartub, K.; Maley, A. M.; Corn, R. M. Fabrication of PEDOT Nanocone Arrays with Electrochemically Modulated Broadband Antireflective Properties. *J. Phys. Chem. Lett*. ***2017***, 8, 576-579.

(19) Shen, W.; Li, Z.; Wang, H.; Liu, Y.; Guo, Q.; Zhang, Y. Photocatalytic Degradation for Methylene Blue using Zinc Oxide Prepared by Codeposition and Sol-Gel Methods. *J. Haz. Mat*. ***2008***, 152, 172-175.

(20) Jang, Y. J.; Simer, C.; Ohm, T. Comparison of Zinc Oxide Nanoparticles and its Nano-Crystalline Particles on the Photocatalytic Degradation of Methylene Blue. *Mater. Res. Bull*. ***2006***, 41, 67-77.

(21) Voss, T.; Svacha, G. T.; Mazur, E.; Konjhodzic D.; Marlow, F. High Order Waveguide Modes in ZnO Nanowires. *Nano. Lett*. ***2007***, 7, 3675-3680.

(22) Kim, S. K.; Song, K. D.; Kempa, T. J.; Day, R. W.; Lieber, C. M.; Park, H. G. Design of Nanowire Optical Cavities as Efficient Photon Absorbers. *ACS Nano* ***2014***, 8, 3707-3714.

(23) Robak, E.; Kotkowiak, M.; Drozdowski, H. Nanostructured Zinc Oxide Systems with Gold Nanoparticle Pattern for Efficient Light Trapping. *J. Phys. D: Appl. Phys*. ***2016***, 49, 045104.

(24) Xu, S.; Adiga, N.; Ba, S.; Dasgupta, T.; Wu, C. F. J.; Wang, Z. L. Optimizing and Improving the Growth Quality of ZnO Nanowire Arrays Guided by Statistical Design of Experiments. *ACS Nano* ***2009***, 3, 1803-1812.

(25) Jheng, B-T.; Liu, P-T.; Wang, M-C.; Wu, M-C. Effects of ZnO-Nanostructure Antireflection Coatings on Sulfurization-Free Cu_2ZnSnS_4 Absorber Deposited by Single-Step Co-Sputtering Process. *Appl. Phys. Lett*. ***2013***, 103, 052904.